0273-2289/02/101/0177/$14.75

Significance of Fluid Regime and Wetted Area in Biofilm Reactors

YILMAZ MUSLU

Department of Environmental Engineering, Faculty of Civil Engineering, Technical University of Istanbul, 80626 Ayazaga, Istanbul, Turkey

Received June 14, 2000; Revised July 26, 2001; Accepted September 27, 2001

Abstract

Mass transfer within microbial films was described using Monod-type biological kinetics in terms of properties of filter media and feed solution. The performance characteristics of a trickling filter were thus modeled. The model enables one to consider the effect of inlet substrate concentration and flow rate upon the removal efficiency. For this purpose a second-order partial differential equation describing the dispersion phenomena inside the liquid layer was solved under special boundary conditions and used to determine substrate flux into the biofilm. A uniform biofilm thickness was considered. The model is based on computer techniques and the numerical evaluation of the normalized biofilm mathematical model. A design procedure was also given to calculate biological filters. The numerical model was also applied to experimental data to demonstrate its validity.

Index Entries: Biological surveys; concentrations; design practices; diffusion; environmental engineering; mass transfer; mathematical models; biological filters; trickling filters.

Introduction

Substrate reduction in fixed film processes such as those in aerobic filters, trickling filters, and rotating disk reactors has been widely used in the application of wastewater treatment technology *(17)*. An understanding of the factors affecting the rates of biofilm reactions is therefore essential in designing wastewater treatment units *(18)*. For this purpose a conceptual model consisting of parallel plates over which a hydraulically controlled biofilm grows was used in this investigation. The microbial film is covered with a liquid film, the wetted surface of which depends on the flow rate and media characteristics. Substrate concentration decreases from the liquid surface to the biofilm surface due to the mass transfer inside the

*Author to whom all correspondence and reprint requests should be addressed.

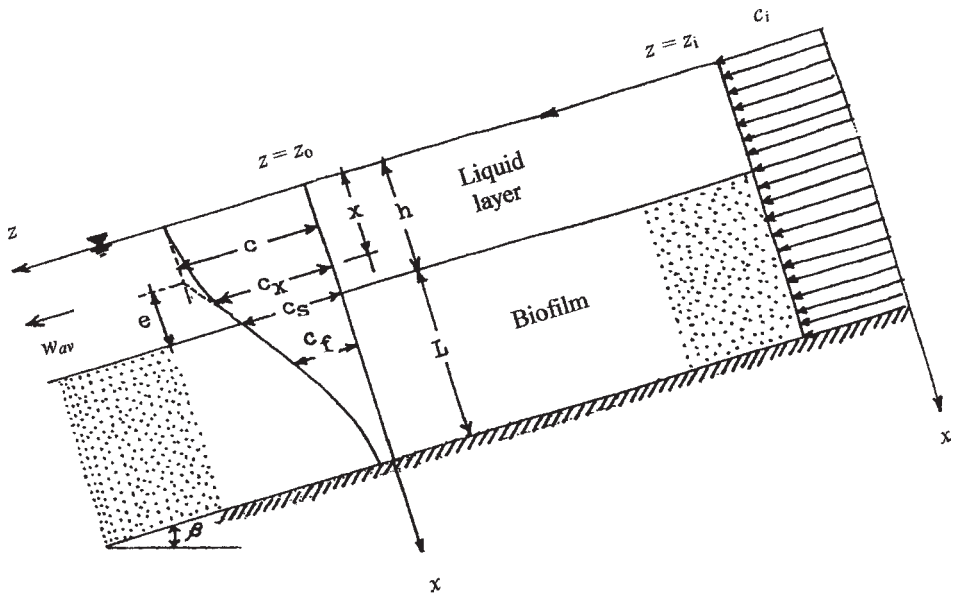

Fig. 1. Substrate distribution in an inclined plane biofilm model.

liquid layer of depth h (Fig. 1). This kinetic model assumes an idealized biofilm which is characterized by a uniform biomass density X_c (M L^{-3}), a uniform depth L (L), and uniform Monod kinetic constants over the entire thickness of the biofilm *(8,10,13)*. Substrate flux N (M L^{-2} T^{-1}) penetrating into the biofilm can be described according to Fick's law as $N = -D_w(dc_x/dx)$ at $x = h$ *(14,15)* in which D_w = molecular diffusivity of substrate in the liquid film, L^2 T^{-1}; x = length dimension normal to biofilm surface, L; c_x = substrate concentration at any location inside the liquid layer, M L^{-3}. Any quantity at the biofilm surface is denoted by the subscript "s," e.g., c_s is the substrate concentration at the biofilm surface. Similarly, c_f is the substrate concentration inside the biofilm. Substrate concentration c_f decreases from the biofilm surface to the attachment surface of the support media due to the substrate use within the biofilm *(4,7)*. Monod kinetics can be used to model the substrate consumption rate *(2,19)*. A mass balance equation between diffusion and reaction using Monod kinetics was solved by Atkinson and Davies *(3)*. A relationship equivalent to its numerical solution was then derived as $N = f(k_1, M, B_s)$ in which f is a hyperbolic function of a coefficient k_1, a dimensionless microbial film thickness $M = k_2 L$ and a dimensionless substrate concentration $B_s = k_3 c_s$ at liquid biofilm interface. [See also Atkinson and Abdel Rahman Ali *(5)*.] The values of k_1, k_2, and k_3 are coefficients defined as the combinations of Monod's kinetic coefficients (see the list of notations). In the special case of thin and thick biofilms, N is directly proportional with B_s for small substrate concentrations:

$$N = \xi c_s \tag{1}$$

in which ξ is a proportionality factor, L T^{-1} as

$$\xi = k_1 L \text{ for thin biofilms } (M \leq 0.5) \quad (2)$$

$$\xi = \frac{k_1}{k_2} \text{ for thick biofilms } (M \geq 3) \quad (3)$$

These are asymptotic forms of the more general kinetic equation mentioned above, which may be, for instance, of zero order, half order, first order, etc., reaction kinetics. The liquid layer is assumed to be void of microorganisms. At the inlet section there is an uniform substrate concentration c_i. Owing to the molecular diffusion and the existence of a velocity gradient, a dispersion phenomenon takes place. The resulting dispersion equation should be solved numerically under the general boundary condition $N = f(k_1,M,B_s)$, the solution of which is extremely complex in this general case. However, for the special cases of thin and thick biofilms with small substrate concentrations (Eq. 1), its solution is simplified. Otherwise, a plug-flow regime should be assumed to simplify the solution for the general boundary condition.

Objectives of this article are (1) to provide a model to determine the substrate removal efficiency for the special boundary conditions (Eq. 1) at any hydraulic loading; (2) to solve the dispersion equation under the general boundary conditions for plug flow regime at low flow rates and develop computer programs to determine substrate removal efficiency as a function of c_i (see Table 1 for the computer output as an example); (3) to compare the results obtained from the two approaches for the same conditions in order to derive general relationships (see Table 2); (4) to study wetting rate and surface effects in filter media; (5) to determine the effect of flow rate on the mass transfer coefficient using the computer programs developed (see Eqs. 15–22); (6) to give further experimental evidence in addition to those given in an earlier paper *(13)*; (7) to develop design principles for biological filter in which substrate removal efficiency decreases with inlet substrate concentrations especially in the case of concentrated wastewater from industry (see *Examples*).

Owing to the extremely complex nature of the problem outlined above, a conceptual model was accepted, which consists of a bundle of vertical plates with an angle of $\beta = 90°$ in which β is the angle of inclined plane with the horizon (Fig. 1). A filter element with a cross-sectional area A and depth l was considered as shown in Fig. 2. If the specific surface area is S, then the surface area of the filter medium is given by $S(AL)$, which should be equal to the wetted area in the conceptual model, namely, as $Bl = S(Al)$ and hence $B = SA$ where B denotes the wetted perimeter. These equations convert the filter medium into a series of parallel plates whose total width is equal to $B = \Sigma b$ in which b is the width of each parallel plane (Fig. 2) The distance Δ between the two vertical planes is equal to S^{-1}. Biofilm thickness is constant for a given flow rate because it is controlled by the shear stress exerted by the flowing liquid on the biofilm. It was further assumed that kinetic coefficients k_1, k_2, and k_3 depend upon substrate–microbe system and are gen-

Table 1
Computer Output for Biological Efficiency in Biofilm Reactors

M= .1 K= .06998 Ao= 3.821
A1= 3.9 ALPHA= 58.489 STEP= .001

Bs	B	dZ	Z	z=Ao*Z cm	c mg/L	Efficiency
0.0010	0.0024	0.0000	0.0000	0.0000	0.0000	0.0000
0.0020	0.0048	18.2275	18.2275	69.6473	0.0012	0.0000
0.0030	0.0073	10.1246	28.3521	108.3333	0.0019	0.0000
0.0040	0.0097	7.0860	35.4380	135.4087	0.0025	0.0000
0.0050	0.0121	5.4654	40.9034	156.2919	0.0031	0.0000
0.0060	0.0145	4.4525	45.3559	173.3049	0.0037	0.0000
0.0070	0.0169	3.7580	49.1139	187.6642	0.0043	0.0000
0.0080	0.0193	3.2516	52.3655	200.0884	0.0049	0.0000
0.0090	0.0217	2.8657	55.2312	211.0383	0.0056	0.0000
0.0100	0.0241	2.5619	57.7930	220.8272	0.0062	0.0000
0.0110	0.0265	2.3163	60.1094	229.6780	0.0068	0.9004
0.0120	0.0289	2.1138	62.2232	237.7547	0.0074	0.8990
0.0130	0.0313	1.9438	64.1670	245.1820	0.0080	0.8984
0.0140	0.0337	1.7991	65.9661	252.0564	0.0086	0.8985
0.0150	0.0360	1.6745	67.6406	258.4546	0.0092	0.8991
0.0160	0.0384	1.5660	69.2065	264.4382	0.0099	0.8999
0.0170	0.0408	1.4707	70.6772	270.0575	0.0105	0.9010
0.0180	0.0432	1.3863	72.0634	275.3544	0.0111	0.9022
0.0190	0.0456	1.3110	73.3744	280.3637	0.0117	0.9034
0.0200	0.0479	1.2435	74.6179	285.1152	0.0123	0.9048
0.0210	0.0503	1.1826	75.8005	289.6338	0.0129	0.9061
0.0220	0.0527	1.1274	76.9279	293.9414	0.0135	0.9071
0.0230	0.0550	1.0770	78.0049	298.0568	0.0141	0.9064
0.0240	0.0574	1.0310	79.0359	301.9963	0.0147	0.9060
0.0250	0.0597	0.9888	80.0247	305.7743	0.0153	0.9057
0.0260	0.0621	0.9498	80.9745	309.4035	0.0159	0.9056
0.0270	0.0644	0.9138	81.8883	312.8951	0.0165	0.9057
0.0280	0.0668	0.8804	82.7687	316.2592	0.0171	0.9059
0.0290	0.0691	0.8494	83.6181	319.5048	0.0177	0.9061
0.0300	0.0715	0.8205	84.4386	322.6398	0.0183	0.9065
0.0310	0.0738	0.7934	85.2320	325.6715	0.0189	0.9069
0.0320	0.0762	0.7681	86.0001	328.6065	0.0195	0.9073
0.0330	0.0785	0.7444	86.7445	331.4508	0.0201	0.9078
0.0340	0.0808	0.7221	87.4666	334.2098	0.0207	0.9076
0.0350	0.0832	0.7010	88.1676	336.8884	0.0213	0.9073
0.0360	0.0855	0.6812	88.8488	339.4911	0.0219	0.9071
0.0370	0.0878	0.6624	89.5112	342.0222	0.0225	0.9070
0.0380	0.0902	0.6447	90.1558	344.4855	0.0231	0.9069
0.0390	0.0925	0.6278	90.7837	346.8844	0.0237	0.9070
0.0400	0.0948	0.6118	91.3955	349.2222	0.0243	0.9070
0.0410	0.0971	0.5967	91.9922	351.5021	0.0249	0.9072
0.0420	0.0994	0.5822	92.5744	353.7266	0.0255	0.9073
0.0430	0.1017	0.5684	93.1428	355.8986	0.0261	0.9075
0.0440	0.1040	0.5553	93.6981	358.0203	0.0267	0.9078
0.0450	0.1063	0.5427	94.2408	360.0941	0.0273	0.9077
0.0460	0.1087	0.5307	94.7715	362.1220	0.0279	0.9075
0.0470	0.1110	0.5193	95.2908	364.1061	0.0284	0.9074
0.0480	0.1133	0.5083	95.7990	366.0481	0.0290	0.9073
0.0490	0.1155	0.4977	96.2968	367.9499	0.0296	0.9072
0.0500	0.1178	0.4876	96.7844	369.8130	0.0302	0.9072
0.0510	0.1201	0.4779	97.2622	371.6390	0.0308	0.9072
0.0520	0.1224	0.4685	97.7308	373.4293	0.0314	0.9073
0.0530	0.1247	0.4596	98.1903	375.1853	0.0320	0.9073
0.0540	0.1270	0.4509	98.6413	376.9083	0.0326	0.9074
0.0550	0.1070	0.4428	99.0841	378.6003	0.0274	0.8883

erally the same for all filters using the same substrate. Although there may be significant differences in biofilm structure depending on the operating conditions, k_1, k_2, and k_3 were assumed to be constant for a given substrate to overcome the mathematical difficulties arising from considering a large number of parameters. However, density/compactness and diffusion effects are indirectly considered by the terms of X_c and D_c appearing in the expressions of k_1 and k_2. The possible error may further be compensated for

Table 2
Ratio of e/h to Calculate Mass Transfer Coefficient E for Different Values of η_D and Z_D

	η_D											
Z_D	0.05	0.10	0.20	0.50	0.75	1.00	2.00	4	6	8	10	100
0.01	0.250	0.251	0.261	0.265	0.267	0.262	0.268	0.276	0.281	0.285	0.288	0.311
0.02	0.308	0.309	0.320	0.313	0.315	0.323	0.331	0.341	0.347	0.352	0.355	0.370
0.04	0.359	0.372	0.377	0.383	0.387	0.389	0.399	0.411	0.418	0.423	0.426	0.442
0.06	0.403	0.408	0.414	0.418	0.426	0.427	0.438	0.450	0.457	0.461	0.464	0.480
0.08	0.424	0.431	0.436	0.444	0.448	0.451	0.462	0.474	0.480	0.484	0.487	0.499
0.10	0.438	0.446	0.451	0.458	0.462	0.466	0.477	0.488	0.494	0.497	0.500	0.510
0.12	0.449	0.456	0.461	0.469	0.473	0.476	0.486	0.497	0.502	0.505	0.507	0.517
0.14	0.449	0.463	0.468	0.475	0.479	0.482	0.492	0.502	0.507	0.510	0.512	0.520
0.16	0.449	0.467	0.472	0.479	0.483	0.487	0.496	0.505	0.510	0.512	0.514	0.522
0.18	0.449	0.470	0.475	0.482	0.486	0.489	0.498	0.507	0.511	0.514	0.516	0.523
0.20	0.449	0.472	0.477	0.484	0.487	0.491	0.500	0.508	0.512	0.515	0.516	0.523
0.26	0.449	0.473	0.480	0.486	0.490	0.493	0.501	0.509	0.513	0.516	0.517	0.523
0.30	0.449	0.476	0.480	0.487	0.490	0.494	0.502	0.510	0.514	0.516	0.517	0.523
0.40	0.449	0.476	0.481	0.487	0.491	0.494	0.502	0.510	0.514	0.516	0.517	0.523
0.50	0.449	0.476	0.481	0.487	0.491	0.494	0.502	0.510	0.514	0.516	0.517	0.523
1.00	0.449	0.476	0.481	0.487	0.491	0.494	0.502	0.510	0.514	0.516	0.517	0.523
1.50	0.449	0.476	0.481	0.487	0.491	0.494	0.502	0.510	0.514	0.516	0.517	0.523
2.00	0.449	0.476	0.481	0.487	0.491	0.494	0.502	0.510	0.514	0.516	0.517	0.523
2.50	0.449	0.476	0.481	0.487	0.491	0.494	0.502	0.510	0.514	0.516	0.517	0.523

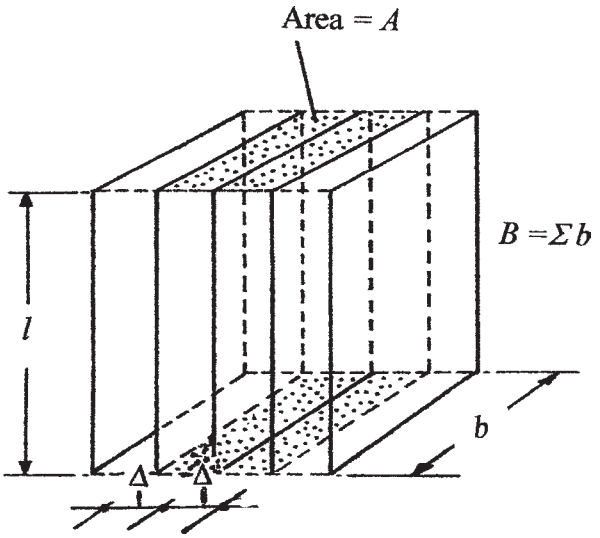

Fig. 2. Conceptual model assumed to study biological filtration.

using experimental values of the coefficients as explained in the evaluation of the experimental data.

Solution to Dispersion Equation for Special Boundary Conditions at Any Flow Rate

In this case a two-dimensional dispersion is under consideration for special boundary conditions (Eq. 1), The following normalizing parameters were used to solve the dispersion equation with the aid of the finite difference method *(10,12)*:

$$C_x = \frac{c_x}{c_i}; C_s = \frac{c_s}{c_i} \tag{4}$$

$$Z_D = \frac{D_w Z}{h^2 w_{max}}; X = \frac{x}{h}; h = \left[\frac{3\mu q}{\gamma \sin\beta}\right]^{1/3} \tag{5}$$

in which w_{max} = maximum value of the parabolic velocity profile w at the liquid surface, L T^{-1}; β = the angle of inclined plane with the horizon; γ = liquid specific gravity, M L^{-2} T^{-2}; μ = dynamic viscosity, M L^{-1} T^{-1}; q = rate of flow per unit width of the biofilm, L^3 T^{-1} L^{-1}. The z-axis is on the liquid surface and parallel to the flow direction. The dimensionless distance Z_D can be found using the physical parameters related to the filter. The value of $Z_D = (Z_D)_o$ for the outlet section is thus obtained substituting the filter length $z = l$ into Eq. 5 as *(13)*

$$Z_D = (Z_D)_o = \frac{D_w l}{h^2 w_{max}} = \frac{D_w l}{h^2 (3/2) w_{av}} = \frac{2}{3} \frac{D_w}{h} \frac{l}{q} \quad (6)$$

in which w_{av} is the mean velocity of the parabolic velocity profile calculated as $(2/3)\, w_{max}$. Equation 1 was then accepted as a boundary condition and the dispersion equation governing the liquid film was solved. Computer techniques and the method of finite differences were used *(9,11)*. Numerical values of dimensionless concentrations $C_x = f(Z_D, X, \eta_D)$ were thus obtained for different values of

$$\eta_D = \frac{\xi}{D_w} h \quad (7)$$

As C_x and C_s are known, the bulk liquid phase substrate concentration C was then obtained from

$$C = \frac{c}{c_i} = \frac{3}{2} \int_{X=0}^{X=1} C_x (1 - X^2)\, dX \quad (8)$$

The theory given above is valid for laminar flow and for a special boundary condition. However, it can be used to obtain a general picture of flow regime and its effect on the concentration variation in the lateral direction. In fact, a family of curves of C_x vs X is obtained for a given value of η_D, the value of Z_D being a parameter. Each curve represents concentration variation with respect to X in a given cross-section for a given value of η_D. For small values of $\eta_D = k_s h / D_w$, i.e., for liquid films of small depths, concentration profiles are flattened. At these low hydraulic loadings with small η_D and large Z_D values, variation of C_x with respect to X may be neglected (plug-flow condition). The concentration profile may then be idealized assuming a bulk concentration, which will be studied below for the general boundary condition.

A Biofilm Mathematical Model for Plug-Flow Conditions

At low hydraulic loadings, dispersion is less significant and a bulk substrate concentration c can be used in place of c_x. In this simple case, the general boundary condition $N = f(k_1, M, B_s)$ can be considered for the plug-flow reactor with no dispersion in the x-direction. This solution should be coincident with the results obtained from Eq. 8 for low hydraulic loadings at thick and thin biofilms when $c_i \to 0$ from which the numerical relationship in Table 2 was derived. For the sake of simplicity, under plug-flow conditions, a bulk liquid phase substrate concentration c at an active liquid thickness h was combined with a stagnant liquid layer of thickness e to express substrate flux

$$N = -D_w \frac{dc_x}{dx} \cong D_w \frac{c - c_s}{e}$$

for $x = h$ at low hydraulic loadings (Fig. 1). Dimensionless distance in the z-direction was denoted by $Z = [k_1/(k_2 q)]z$ in this case. Dimensionless filter length α in which substrate concentration is reduced from any initial value of B_{si} (or B_i) to an outlet concentration of B_{so} (or B_o) is

$$\alpha = Z_o - Z_i = \frac{k_1 L}{k_2 L}\frac{l}{q} = \frac{k_1 L}{M}\frac{l}{q} \tag{9}$$

in which Z_o and Z_i are dimensionless distances for outlet and inlet sections measured from an origin. There is a relationship between substrate reduction ΔB_s and the dimensionless distance ΔZ as shown in Table 1. A differential substrate mass balance equation was therefore written for the liquid layer and numerically solved for substrate removal efficiency η under consideration of general boundary condition $N = f(k_1, M, B_s)$. For this purpose a computer program was developed *(13)*. The biological efficiency $\eta = 1 - (B_o/B_i)$ or $1 - (c_o/c_i)$ corresponding to a given inlet concentration B_{si} (or B_i) was obtained when four input data, namely, M, $A_1 = 10^{-6} k_3$, α, and $K = (D_w/e)(k_2/k_1) = E(k_2/k_1)$ are given as shown in Table 1 in which $E = D_w/e$ is a mass transfer coefficient. An additional input datum of $A_o = (k_2/k_1)q = l/\alpha$ is also required if dimensional distance z for a given substrate reduction is to be determined. In general, it is sufficient to express η as a function of B_i (dimensionless) or c_i (mg L^{-1}) for practical purposes. Therefore, there is no need to know A_o in this case. Under asymptotical conditions for low and high concentrations, analytical solutions can be obtained in place of numerical integration in Table 1. When c_i tends to zero, for example, the following analytical result is obtained *(5)*:

$$\ln \frac{c_o}{c_i} = \ln (1 - \eta_o) = -\frac{K \tanh M}{K + \tanh M}\alpha \tag{10}$$

in which $\eta_o = 1 - (c_o/c_i)$ is the value of η for $c_i \to 0$. For thin biofilms ($M \leq 0.5$) Eq. 10 becomes

$$\ln \frac{c_o}{c_i} \cong -\frac{K}{\frac{K}{M} + 1}\alpha \tag{11}$$

On the other hand, for all values of M, when c_i is sufficiently large, numerical integration reduces to the following analytical solution:

$$\eta = 1 - \frac{c_o}{c_i} = \frac{k_1 L}{k_3}\frac{l}{q}\frac{1}{c_i} = I\frac{1}{c_i} \tag{12}$$

in which

$$I = \frac{k_1 L}{k_3}\frac{l}{q} = \frac{k_1 L}{k_3}\frac{l}{q}\frac{k_2 L}{k_2 L} = \frac{M}{k_3}\alpha \tag{13}$$

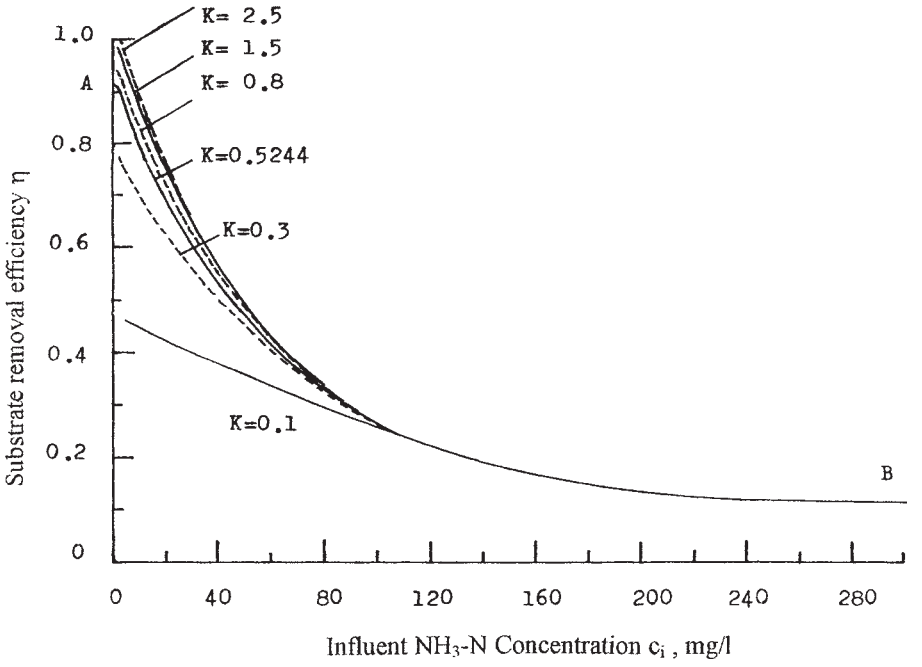

Fig. 3. The effect of mass transfer parameter K on substrate removal efficiency η (based on the data of Atkinson and How, ref. *4*; $m = 16.02$, $A_1 = 4.315\ cm^3\ g^{-1}$, $\alpha = 6.846$).

If the experimental data are replotted in terms of η vs $1/c_i$, the result is a linear relationship at high concentrations with a slope of I. When c_i tends toward zero, for low hydraulic loadings in thick and thin biofilms, Eq. 8 also gives an asymptotic solution to the numerical integration in Table 1 which can be used to obtain the ratio of e/h and mass transfer coefficient $E = D_w/e$. The resulting values were given in Table 2.

Example 1

In a biofilm reactor with a length of $l = 204.5$ cm, fractional conversion η was measured in terms of NH_3 – N removal over the range of influent concentrations of 4.8 to 204.0 mg L^{-1} as follows:

c_i (mg/L):	4.8	13.1	24.0	39.3	48.7	70.9	81.1	120.6	204.0
η:	0.85	0.739	0.633	0.541	0.487	0.348	0.309	0.209	0.124

(i) Calculate the value of k_1 assuming that the value of $c_i = 204$ mg/L is a concentration sufficiently large and that the corresponding removal efficiency is η = 0.124 (Point B in Fig. 3).

(ii) If the points plotted with the given data lie on a curve of η vs c_i with a limiting efficiency of $\eta_o = 0.905$ for $c_i \rightarrow 0$ (Point A in Fig. 3), find the value of K [$k_2 = 133.5\ cm^{-1}$, $k_3 = 4.315 \times 10^6\ cm^3\ g^{-1}$, thick biofilm, $L = 0.12$ cm and $q = 4.77 \times 10^{-2}\ cm^3\ cm^{-1}s^{-1}$].

Solution

(i) $c_i = 204$ mg $l^{-1} = (204)(10^{-3})$ g $l^{-1} = (204)(10^{-6})$ g cm^{-3}; Eq. 12 leads to

$$\eta = \frac{k_1 L}{k_3}\frac{l}{q}\frac{1}{c_i} = \frac{(k_1)\,(0.12)\,(204.5)}{(4.315)\,(10^6)\,(0.0477)}\frac{1}{(204\times10^{-6})} = 0.124 \rightarrow k_1 = 0.2129\text{s}^{-1}$$

Therefore, the value of I for large concentrations is

$$I = \frac{k_1 L}{k_3}\frac{l}{q} = \frac{0.2129\times0.12}{4.315\times10^6}\times\frac{204.5}{0.0477} = 2.538\times10^{-5}\text{ g cm}^{-3}$$

(ii) The value of K is estimated from Eqs. 9 and 10:

$$\alpha = \frac{k_1 l}{k_2 q} = \frac{0.2129\times204.5}{133.5\times0.0477} = 6.846$$

$$\frac{c_o}{c_i} = 1 - 0.905 = 0.095;\ \text{In } 0.095 = -\frac{K\tanh 16.02}{K+\tanh 16.02}\times 6.846 \rightarrow K = 0.5244$$

Other input parameters for the computer program are

$$M = k_2 L = 133.5\times0.12 = 16.02;\ A_1 = 10^{-6}\,k_3 = 10^{-6}\times4.315\times10^6 = 4.315\text{ cm}^3\text{ g}^{-1}$$

The computer program was performed using these input data and the value of η obtained were plotted against c_i (solid line in Fig. 3 for $K = 0.5244$). A good agreement was obtained between the computed and observed values. (Experimental points were not shown in Fig. 3 to keep the figure uncomplicated.)

Effect of Input Parameters

Input data of M, A_1, and α can be calculated using equations given earlier, if the values of L, l, and q are given in addition to the constant values of the kinetic coefficients k_1, k_2, and k_3, The fourth input parameter K, however, can only be found if at least one point of the curve η vs c_i is given. All necessary parameters are thus obtained to perform the computer program for a given flow rate. If K changes while M, A_1, and α remain constant, η vs c_i curves pass through the same point B for large concentrations as shown in Fig. 3 because all parameters in Eq. 12 remain unchanged. Although the predicted values of η are under the influence of K at the beginning of these curves, the effect of K on η is generally not great because the values of mass transfer coefficients are very high for flow rates in the practical ranges of liquid applications. Therefore, the liquid phase mass transfer resistance may be assumed to be negligible in those cases. The effect of K on η was demonstrated evaluating the experimental results published by Atkinson and How *(4)* for a flow rate per unit width q = (4.77) (10^{-2}) cm^3 cm^{-1}s^{-1}. In these experiments, the kinetic coefficients of $k_1 = 0.2129$ s^{-1},

$k_2 = 133.5\ \text{cm}^{-1}$, and $k_3 = (4.315)(10^6)\ \text{cm}^3\ \text{g}^{-1}$ for a NH_3-N feed solution were measured with a thick biofilm of depth $L = 0.12$ cm and of length $l = 204.5$ cm. The fractional conversion η was measured in terms of NH_3-N removal and a value of $\eta_o = 0.905$ was given for $c_i \to 0$ (Point A in Fig. 3). The correct value of K should be determined from the observed values of η. Other input data are $M = k_2 L = (133.5)(0.12) = 16.02$;

$$A_1 = 10^{-6}\, k_3 = (10^{-6})(4.315)(10^6) = 4.315\ \text{cm}^3\ \text{g}^{-1};\ \alpha = -\frac{k_1 l}{k_2 q} = \frac{0.2129}{133.5}\,\frac{204.5}{0.0477} = 6.846$$

and $A_o = l/\alpha = 204.5/6.846 = 29.87$l. The value of K was therefore estimated from Eq. 10:

$$\frac{c_o}{c_i} = 1 - 0.905 = 0.095;\ \text{In}\ 0.095 = -\frac{K \tanh 16.02}{K + \tanh 16.02} \times 6.846 \to K = 0.5244$$

The computer program used these input data and the values of η obtained were plotted against c_i (solid line in Fig. 3 for $K = 05244$). They are in good agreement with the measured substrate removal efficiencies. (Experimental points were not shown in Fig. 3 to keep the figure uncomplicated.) The value of $K = 0.5244$ is therefore correct. The effect of K on η was further investigated in a large interval when K varied from $K = 0.1$ to $K = 2.5$ for the same flow rate. The results obtained from the computer program were also plotted in Fig. 3 against c_i. Each curve in Fig. 3 has a point of intersection with the vertical axis that can also be obtained from Eq. 10. As an example, for $K = 0.8$ it becomes

$$\text{In}\,\frac{c_o}{c_i} = -\frac{0.8 \tanh 16.02}{0.8 + \tanh 16.02} \times 6.846 \to \frac{c_o}{c_i} = 0.0477;\ \eta_o = 1 - \frac{c_o}{c_i} = 1 - 0.0477 = 0.9523$$

A study of Fig. 3 indicates that the effect of K on η is not great for values of K close to or larger than the actual value, $K = 0.5244$. If this example is repeated with a thin biofilm, it can be observed that the effect of K on η is even smaller in this case. In order to obtain the curves of η vs c_i for other flow rates, the corresponding input data for the computer program should be determined. M and A_1 do not change with q. The other input parameters, α and K, however, are influenced by flow rate. Although the effect of K on η was studied above, it is necessary to determine the variation of K and α with unit width discharge q for design purposes as discussed below.

Flow Characteristics and Structure of the Media

The most important characteristics of filter media are specific surface area and porosity. The media surface area divided by the volume of the container is called the specific surface area S. Biological filters consist of various types of plastic packings and natural materials such as crushed stones. Owing to the complex nature of the filter media, conceptual models

as mentioned earlier are used to study the flow phenomena. Plastic packings have plane surfaces in good agreement with the model used. Natural materials, however, can only be studied using the conversion formula given below. Specific surface area of the plastic packings are given by their manufacturers. Plastic *surfpac* medium, for instance, has a specific surface of S = 28 ft^2/ft^3 (= 91.9 m^2/m^3) with a void volume of 95%. A synthetic media of *floccor* packing, on the other hand, has a specific surface of S = 85 m^2/m^3. The specific surface area of natural media depends upon shape, size, and the arrangement of the grains. For cubical and rhombic arrangements of spheres, it becomes $S = \pi/2a$ and $S = 4.44/2a$, respectively, in which a is the radius of sphere. Specific surface area of a randomly packed assemblage of spheres can be expressed by $S = 6(1 - \varepsilon)/2a$, in which ε is porosity *(10)*. A value of $\varepsilon = 0.40$ may be accepted for the porosity of randomly packed media. Under this assumption, the specific surface area of randomly packed media may thus be obtained from $S = 6(1 - \varepsilon)/2a = 6(1 - 0.4)/2a = 3.6/2a$. The specific surface defined above is for a dry filter, i.e., before liquid application. Owing to the wetting and channeling effects, this definition should be modified to give the wetted area *(6)*. Using a proportionality constant ψ, the wetted specific surface area S_w can be defined as $S_w = \psi S$. The specific surface being determined in this way, flow characteristics can be obtained from the conceptual model.

For this purpose consider a filter element with a cross-sectional area A and depth l. If the wetted specific surface area of the filter medium is S_w, the wetted surface area of the filter bed is given by $(S_w)(Al)$, which equates the wetted area as follows: $b_w\, l = (S_w)(Al) \rightarrow b_w = S_w\, A = \psi SA = \psi\, b$, in which b_w is the wetted perimeter and $b = SA$ *(13)*. Thus, the flow rate per unit width q_w ($L^3\, T^{-1}\, L^{-1}$) is

$$q_w = \frac{Q}{b_w} = \frac{Q}{S_w A} = \frac{Q/A}{S_w} = \frac{Q_A}{\psi S} = \frac{q}{\psi} \tag{14}$$

in which Q = volumetric flow rate, $L^3\, T^{-1}$, Q_A = hydraulic loading rate, $L\, T^{-1}$, and $q = Q/b = Q_A/S$, $L^2\, T^{-1}$. These equations convert the filter media into a series of parallel plates. The total width of these parallel plates covered with liquid is equal to b_w.

The flow rate q_w can be obtained from Eq. 5 as $q_w = (\gamma \sin\beta/3\mu)\, h^3$ from which results

$$q = \psi\, q_w = \psi\, (\gamma \sin\beta/3\mu)\, h^3 = \psi\, (\text{constant})\, h^3$$

$$\frac{q_1}{q_2} = \frac{\psi_1}{\psi_2}\frac{h^3}{h_2^3} \tag{15}$$

in which the subscripts 1 and 2 denote the values corresponding to flow rates q_1 and q_2, respectively. The liquid film was assumed to follow the contours of the packing materials; h = depth of active liquid film in media

depressions and contributes to flow. Conditions similar to "depression storage" may be observed. It is reasonable to accept that the wetted area in the filter bed increases with the liquid film thickness, since in this case more area will be covered by the liquid. Therefore, the assumption of $(\psi)_1/(\psi)_2 = (h)_1/(h)_2$ was made to obtain the following general relationship from Eq. 15 for the variation of the wetted surface area with the flow rate *(13)*

$$\frac{\psi_1}{\psi_2} = \frac{h_1}{h_2} = \left(\frac{q_1}{q_2}\right)^{1/4} \tag{16}$$

or

$$\psi_2 = \psi_1 = \left(\frac{q_2}{q_1}\right)^{1/4} \tag{17}$$

Now flow dependence of α and K for a given substrate can be determined using Eqs. 15–17. The parameter α_2 is obtained from Eqs. 9 and 14

$$\alpha_2 = \frac{k_1 L}{k_2 L}\frac{l_2}{(q_w)_2} = \frac{(\psi_2 k_1 L)}{k_2 L}\frac{l_2}{q_2} \tag{18}$$

Substitution of Eq. 17 into Eq. 18 leads to

$$\alpha_2 = \frac{\psi_1 k_1 L\,(q_2/q_1)^{1/4}}{k_2 L}\frac{l_2}{q_2} \tag{19}$$

Similarly the effect of flow rate on the parameter K can be investigated using Eq. 14:

$$E = \frac{D_w}{e}\,;\; K = E\frac{k_2}{k_1} = \frac{D_w}{e}\frac{k_2}{k_1} = \frac{D_w}{e}\frac{k_2 L}{k_1 L} = \frac{D_w}{e}\frac{M}{k_1 L} \tag{20}$$

A study of Table 2 indicates that the values of e/h do not substantially vary and remain unchanged around 0.5 especially for large values of Z_D and η_D in the practical range of liquid application (plug-flow regime). If the ratio of e/h is thus assumed constant, K becomes inversely proportional with liquid depth h, because the other parameters of D_w, k_1, and k_2 remain unchanged. The value of K_2 for the flow rate q_2 then becomes

$$K_2 = K_1\left(\frac{q_1}{q_2}\right)^{1/4} \tag{21}$$

If no experimental data except D_w are available, K can be obtained from Eq. 20 assuming $e_2/h_2 = 0.5$. In this case h_2 for q_2 is first calculated. The value of K is then obtained from

$$e = 0.5h_2 \; ; K_2 = \frac{\frac{D_w}{e_2}k_2}{k_1} = \frac{\frac{D_w}{0.5h_2}k_2}{k_1} = \frac{2D_w}{h_2}\frac{k_2}{k_1} \tag{22}$$

Example 2

In order to see the effect of α and K on η more clearly, the curves of η vs c_i were also obtained for q_2 = 0.035 and q_3 = 0.02 cm^3 cm^{-1} s^{-1}, as an example, based upon the input data of the experimental results of Atkinson and How *(4)*. The input data for $q_1 = 0.0477$ cm^3 cm^{-1} s^{-1} were already given earlier as $\psi_1 k_1 = 0.2129$ s^{-1}; $k_2 = 133.5$ cm^{-1}; $\alpha_1 = 6.846$, and $K_1 = 0.5244$. The input data for q_2 = 0.035 cm^3 cm^{-1} s^{-1} were first calculated using Eqs. 19 and 21:

$$\alpha_2 = \frac{0.2129\left(\frac{0.035}{0.0477}\right)^{0.25}}{133.5} \times \frac{204.5}{0.035} = 8.6240$$

$$K_2 = 0.5244\left(\frac{0.0477}{0.035}\right)^{0.25} = 0.5666, \; (A_o)_2 = \frac{I}{\alpha_2} = \frac{204.5}{8.624} = 23.713$$

Values of $\alpha_3 = 13.122$, $K_3 = 0.6517$ and $(A_o)_3 = 15.585$ were also calculated for q_3 = 0.02 cm^3 cm^{-1} s^{-1} similarly. Values of η obtained from the computer program for these input parameters were plotted in Fig. 4 against c_i. A study of Figs. 3 and 4 indicates that the curves of η vs c_i are influenced by α rather than K when flow rates change for a given substrate.

Experimental Confirmation

To support the theory developed here, further verifications may be desirable for the validity of the equations derived in this section, although Eq. 16 and 17 were experimentally confirmed earlier by Muslu *(13)*. The data supplied from Atkinson and Williams *(2)* and Atkinson and Abdel Rahman Ali *(5)* were used for this purpose to determine the removal efficiencies η for another filter *(13,16)*. The same glucose feed solution was applied to both filters in these experiments. In the first filter, a packed bed of wooden spheres with a diameter of $2a = 5.08$ cm ($S_1 = 0.712$ cm^{-1}) was used to develop a thick microbial film. Depth of the filter was l_1 = 60.96 cm. Removal efficiencies η measured for hydraulic loading rates of $Q_A = 0.0148$, 0.027, 0.054, and 0.081 cm^3 cm^{-2} s^{-1} were evaluated *(13)*. The value of k_3 = (1.706)(10^5) cm^3 g^{-1} obtained by Atkinson and Daoud *(1)* from thin biofilm experiments for the same glucose feed solution was used in this evaluation. Using these input data and the computer program developed, values of η

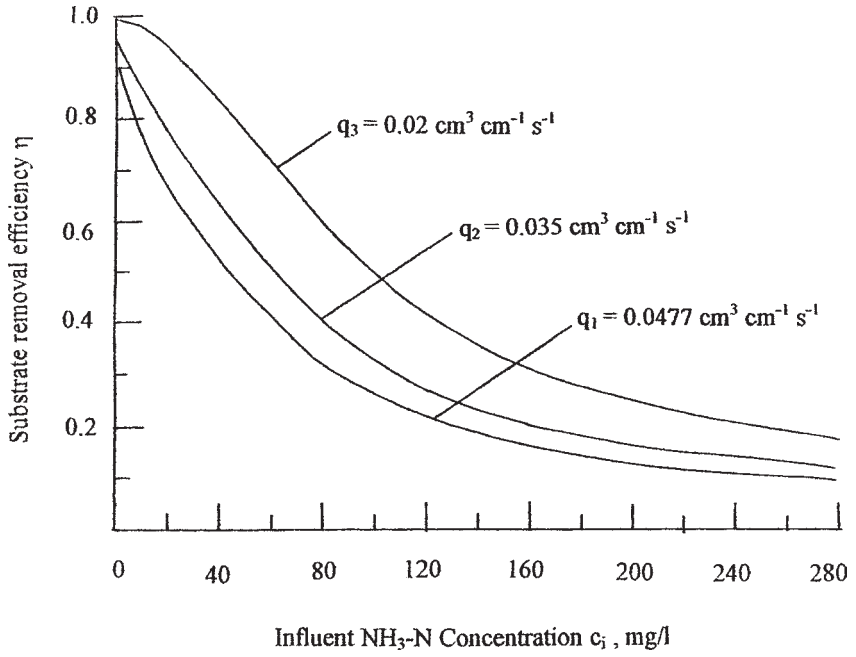

Fig. 4. Effect of flow rate per unit width q on substrate removal efficiency η (based on the kinetic data of Atkinson and How, ref. *4*).

were calculated and plotted against c_i. Good agreement was obtained between the measured and predicted values. Input data obtained from this investigation for $(Q_A)_1 = 0.0148$ cm^3 cm^{-2} s^{-1} were given below as a basis to study substrate removal efficiency η for the second filter:

$$(q)_1 = \left(\frac{Q_A}{S}\right)_1 = \left(\frac{0.0148}{0.712}\right) = 0.02079 \text{ cm}^3 \text{ cm}^{-1} \text{ s}^{-1} ; \psi_1 k_1 L = 0.00448 \text{ cm}^2 \text{s}^{-1} \text{ cm}^{-3} ;$$

$$M = k_2 L = 8.4909; \alpha_1 = 1.5499; K_1 = 6.4088; A_1 = 0.1706 \text{ cm}^3 \text{ g}^{-1}$$

In the second filter bed, plastic spheres of 36.8 mm diameter were contained in a cylinder of 35.4 cm diameter with a depth of $l_2 = 165$ cm ($S_2 = 0.966$ cm^2 cm^{-3}) *(10,16)*. The performance of this filter was investigated at flow rates of 0.962 – 82.64 cm^3 s^{-1}. Filter efficiencies η were measured in terms of COD concentrations (which can be accepted as equal to glucose concentration in mg l^{-1}) and results were given in Table 3. Values of η for this filter can be predicted using the input parameters of the first filter of Atkinson and Williams *(2)*. For this purpose the input data for the second filter were calculated using Eqs. 19 and 21. Results obtained from the computer program for these input data were compared with the measured values in Table 3. This comparison was made below for a hydraulic loading rate of $(Q_A)_2 = 0.005033$ cm^3 cm^{-2} s^{-1} [unit width discharge of $q_2 = (Q_A/S)_2 =$

Table 3
Measured and Predicted Filter Performance Under Various Experimental Conditions

Run	Rate of flow ($cm^3\ s^{-1}$)	Measured COD: Influent c_i ($mg\ L^{-1}$)	Measured COD: Effluent c ($mg\ L^{-1}$)	COD removal efficiency, η: Measured	COD removal efficiency, η: Predicted	$q = Q_A / S$ ($cm^3\ cm^{-1}\ s^{-1}$)	Hydraulic loading rate, Q_A ($cm^3\ cm^{-2}\ s^{-1}$)
4	4.950	840.9	307.5	0.634	0.683	0.00521	0.005033
6	9.900	748.8	403.2	0.462	0.460	0.01040	0.010050
9	25.64	504.0	345.6	0.314	0.316	0.02700	0.026080
11	74.07	546.0	452.4	0.171	0.138	0.07800	0.075350

(0.005033/0.966) = 0.00521 $cm^3\ cm^{-1}\ s^{-1}$, Run No. 4 in Table 3] for purpose of illustration. From Eq. 19 and Eq. 21 it results

$$\alpha_2 = \frac{\psi_1 k_1 L\,(q_2/q_1)^{0.25}}{k_2 L}\frac{l_2}{q_2} = \frac{0.004487\left(\frac{0.00521}{0.02079}\right)^{0.25}}{8.4909}\frac{165}{0.00521} = 11.841$$

$$K_2 = 6.4088\left(\frac{0.02079}{0.00521}\right)^{0.25} = 9.067$$

Other input data are M = 8.4909; A_1 = 0.1706 $cm^3 g^{-1}$; $A_o = l_2/\alpha_2$ =165/11.841 = 13.935. Computer input data were also calculated for other flow rates similarly and values of η obtained from the computer program were given in Table 3 for purpose of comparison. A study of Table 3 indicates that the predicted substrate removal efficiencies η are in good agreement with the measured ones.

Summary and Conclusions

Substrate utilization in random-media trickling filters was described using Monod-type rate equations and mass transfer concepts. The model enables one to take into account the effects of influent substrate concentrations and flow rates on removal efficiencies. In this model biofilm thickness was assumed to be controlled by shear stress due to the water flowing on the biofilm. Computer techniques were first developed for numerical evaluation of a normalized biofilm mathematical model. A linear relationship justified by experimental findings was used for the variation of wetted surface. This was accounted for by using a wetting coefficient ψ and a mass transfer coefficient *E* in the model when the flow regime is laminar with the flattened concentration distribution of the plug flow. A design procedure was developed for the calculation of biological filters. The theory was experimentally confirmed and its practical application was demonstrated using literature data.

Notation

a = radius of sphere, L
A = cross sectional area, L^2
B_s = dimensionless substrate concentration at liquid biofilm interface
C = dimensionless substrate concentration defined as c/c_i
C_x = dimensionless concentration defined as c_x/c_i
c = bulk substrate concentration, M L^{-3}
c_x = substrate concentration at any location in liquid phase, M L^{-3}
c_f = substrate concentration within biofilm, M L^{-3}
D_c = the diffusivity of substrate in the biofilm, $L^2\ T^{-1}$
D_w = molecular diffusivity of substrate in liquid, $L^2\ T^{-1}$

h = liquid film thickness, L
K = dimensionless ratio of mass transfer rate to kinetic rate
K_s = Monod-half velocity coefficient, M L^{-3}
k = maximum utilization rate of rate limiting substrate, T^{-1}

$k_1 = \frac{kX_c}{K_s}$ = a biological rate equation coefficient, T^{-1}

$k_2 = \left(\frac{k_1}{D_c}\right)^{1/2}$ = a coefficient related to a solid phase diffusional limitation, L^{-1}

$k_3 = 1/K_s$ = a biological rate equation coefficient, M^{-1} L^{-3}
L = microbial film thickness, L
l = dimensional filter length, L
M = dimensionless biofilm thickness
N = substrate flux, M L^{-2} T^{-1}
q = flow rate per unit width of the biofilm, L^3 T^{-1} L^{-1}
Q = volumetric flow rate, L^3 T^{-1}
Q_A = hydraulic loading rate, L^3 T^{-1} L^{-2}
S = specific surface area, L^2 L^{-3}
w_{av} = average velocity of liquid in z direction, L T^{-1}
w_{max} = maximum velocity at the liquid surface, L T^{-1}
X_c = microbial density within biofilm, M L^{-3}
x = distance measured normal to the flow direction, L
z = axial distance measured in flow direction from origin, L
α = dimensionless filter length
γ = liquid specific gravity, M L^{-2} T^{-2}
η = biological removal ratio = biological efficiency

$\eta_D = \frac{\xi}{D_w} h$ = a parameter to express C_x as a function of Z_D and X

μ = dynamic viscosity, M L^{-1} T^{-1}
ψ = proportionality constant to express wetting rate, dimensionless
ξ = a proportionality factor in Eq. 1, L T^{-1}

References

1. Atkinson, B. and Daoud, I. S. (1970), *Trans. Inst. Chem. Engrs.* **48,** 245–254.
2. Atkinson, B. and Williams, D. A. (1971), *Trans. Inst. Chem. Engrs.* **49,** 215–224.
3. Atkinson, B. and Davies, I. J. (1974), *Trans. Inst. Chem. Engrs.* **52,** 248–259.
4. Atkinson, B. and How, S. Y. (1974), *Trans. Inst. Chem. Engrs.* **52,** 260–268.
5. Atkinson, B. and Abdel Rahman Ali, M. E. (1976), *Water Res.* **12,** 147–156.
6. Crine, M., Schlitz, M., and Vandevenne, L. (1991), *Chem. Eng. J.* **46,** B59–B68.
7. Hinson, X. and Kocher, Y. (1996), *J. Environ. Engrg. ASCE* **122(11),** 1023–1030.
8. Muslu, Y. (1983), *Water Res.* **17(1),** 105–115.
9. Muslu, Y. and Sansarcı, H. (1983), Calculation of substrate removal efficiency in biological filters using a numerical approach (in Turkish), *Çevre 83 Sempozyumu*, Dokuzeylul Üniv. Muh. Mim. Fak., Bornova, Izmir, Turkey.

10. Muslu, Y. (1984), *J. Environ. Engrg. ASCE* **110(5),** 961–975.
11. Muslu Y. and Ürun H. (1986), *ITU Dergisi* **44(l–2),** 43–48.
12. Muslu, Y. (1993), *J. Chem. Tech. Biotech.* **57(2),** 127–135.
13. Muslu, Y. (1995), *J. Environ. Engrg. ASCE* **121(1),** 66–83.
14. Parker, D. S. (1999), *J. Environ. Engrg: ASCE* **125(7),** 618–625.
15. Rittman, B. E. and McCarty, P. L. (1981), *J. Environ. Engrg. Div. ASCE* **107(4),** 889–900.
16. Sekerdag, N. and Muslu, Y. (1986), One dimensional dispersion in biological filters, Part II (in Turkish). Doga TU Müh. Ve Çev. D. (TÜB_TAK), Ankara, Turkey, **10(3),** 298–307.
17. Suidan, M. T. (1986), *J. Environ. Engrg. ASCE* **112(1),** 78–93.
18. Suidan, M. T., Rittman, B. E., and Traegner, U. K. (1987), *Water Res.* **21(4),** 491–498.
19. Williamson, K. and McCarty, P. L. (1976), *J. Water Pollution Control Fed.* **48(1),** 9–24.